Fish and Shellfish Immunology 87 (2019) 478–489

Contents lists available at ScienceDirect

Fish and Shellfish Immunology

journal homepage: www.elsevier.com/locate/fsi

Full length article

Genome-wide identification of Toll-like receptors in the Chinese soft-shelled turtle *Pelodiscus sinensis* and expression analysis responding to *Aeromonas hydrophila* infection

Tengfei Liu, Yawen Han, Shulin Chen*, Huiying Zhao**

College of Veterinary Medicine, Northwest A&F University, Yangling, Shaanxi Province, 712100, China

ARTICLE INFO

Keywords:
Chinese soft-shelled turtle *Pelodiscus sinensis*
Toll-like receptor
Immune response
Gene expression
Aeromonas hydrophila

ABSTRACT

Toll-like receptors (TLRs) recognizing specific pathogen-associated molecular patterns play crucial roles in immune defence against pathogen invasion. Although recent advances in many species have reported the characterization and functional roles of TLRs in innate immunity, systematic knowledge of TLRs is still lacking in the Chinese soft-shelled turtle *Pelodiscus sinensis*. In this study, a genome-wide search was performed and identified 15 candidate *PsTLR* family genes in *P. sinensis*. Protein structure analysis revealed the conserved domain arrangements for these PsTLR proteins. Phylogenetic analysis indicated the evolutionary conservation of TLRs among various species. Additionally, a putative interaction network among PsTLR proteins was proposed and several functional partner proteins involved in TLR signalling pathway were predicted in *P. sinensis*. Expression profiling showed that these *PsTLRs* exhibited constitutive expression patterns in different tissues of *P. sinensis*. Moreover, several genes were highly expressed in the major immune organ spleen. Remarkably, the mRNA levels of *PsTLR2-1*, *PsTLR4* and several TLR signalling molecules were significantly up-regulated in the spleen after *Aeromonas hydrophila* infection, indicating that *PsTLRs* and these genes responded to bacterial stress. These results provide rich information for the functional exploration of PsTLRs and will facilitate uncovering the molecular mechanisms underlying immune regulation in *P. sinensis*.

1. Introduction

Innate immunity is a universal and evolutionarily conserved immune system at the front line of host defence against invading pathogens [1]. In multicellular organisms, innate immunity relies on pattern recognition receptors (PRRs) to detect microbial components and to discriminate non-self-substances [2]. As a major group of PRRs, the Toll-like receptors (TLRs) play vital roles in activating the protective innate immune responses by sensing series of pathogen-associated molecular patterns (PAMPs) [3,4]. TLRs are single-pass type I integral membrane glycoproteins that typically consist of multiple extracellular leucine-rich repeat (LRR) domains, a helical transmembrane domain and an intracellular Toll/interleukin-L receptor (TIR) domain [1,5]. The LRR domains enable TLRs to recognize PAMPs and transmit signals to the TIR domain, which recruits intracellular adapter proteins, such as myeloid differentiation factor 88 (MyD88) [2,3]. The TLR signalling via MyD88-dependent or MyD88-independent pathways directs the innate immune responses and results in the stimulation of antimicrobial genes and the production of inflammatory cytokines, such as interleukin (IL), tumour necrosis factor (TNF), type I interferon (IFN) and chemokines [1,3].

Within the animal kingdom, the number of TLR genes varies among different species. In invertebrates, the TLR family spans from 222 genes in the sea urchin to only 2 genes in the ascidian [6–9]. However, less extensive TLR genes are found in vertebrates, which generally have 10-13 gene members [10,11]. Generally, vertebrate TLRs can be categorized into six major subclasses (TLR1, TLR3, TLR4, TLR5, TLR7 and TLR11), and each species usually contains at least one member from each subclass [10]. Functional studies have found that each TLR subclass recognizes a set of PAMPs, including glycolipids, lipoproteins,

---

Abbreviations: Toll-like receptor, TLR; pattern recognition receptor, PRR; pathogen-associated molecular pattern, PAMP; leucine-rich repeat, LRR; Toll/interleukin-L receptor, TIR; myeloid differentiation factor 88, MyD88; interleukin, IL; tumour necrosis factor, TNF; neighbourhood-joining, NJ; quantitative real-time PCR, qRT-PCR

[*] Corresponding author.

[**] Corresponding author.

E-mail addresses: liutf@nwafu.edu.cn (T. Liu), hanyawen185@163.com (Y. Han), csl_1359@163.com (S. Chen), zhaohuiying@nwsuaf.edu.cn (H. Zhao).

https://doi.org/10.1016/j.fsi.2019.01.052
Received 23 November 2018; Received in revised form 23 January 2019; Accepted 30 January 2019

flagellin and nucleic acids [3,10]. Considering the essential roles of TLRs in innate immunity, the molecular forms and biological roles of TLRs have been investigated extensively in many species, especially mammals. Moreover, most studies were conducted in human and mouse, which demonstrates the diverse susceptibility of TLRs to various experimental infections [12]. For instance, mice lacking TLR2 are highly susceptible to infection with *Staphylococcus aureus*, indicating a potentially important role for TLR2 in response to bacterial stress [13–15]. Additionally, mammalian TLR4 can respond to gram-negative bacteria and can recognize the extracellular lipopolysaccharide (LPS), subsequently associating with myeloid differentiation protein 2 (MD2) to activate proinflammatory-related genes [16–18]. Although the characteristics and evolution of TLRs have been widely studied in mammals, the deficient information on the structure, function and expression of TLRs in reptiles limits our knowledge of vertebrate TLRs.

The Chinese soft-shelled turtle *Pelodiscus sinensis*, belonging to the reptiles (family Trionychidae), is one of the most important commercially cultured aquaculture species in Asian countries, especially in China, Japan and Korea. This species is well adapted to an aquatic environment and is famous for its high nutritional and pharmacological values [19]. Furthermore, *P. sinensis* occupies a central position in the evolution of vertebrate, providing a link between ectothermic anamniotic animals (fishes and amphibians) and endothermic amniotic animals (birds and mammals) [20]. Therefore, it can serve as an important model animal in the scientific research works of genetic evolution, phylogeny and biodiversity. In recent years, the rapid expansion and intensification of aquaculture have caused the farm raising of *P. sinensis* to experience serious economic losses due to infectious diseases caused by bacteria [21,22]. *Aeromonas hydrophila*, a ubiquitous waterborne bacterium, represents one of the most common and critical aetiologic agents of diseases in many aquatic animals, including *P. sinensis* [23,24]. Extensive evidence has demonstrated that infection with *A. hydrophila* results in various diseases in *P. sinensis* [22–24]. It is well known that TLRs are responsible for immune responses against microbial infection [25]; thus, a greater understanding of TLRs in *P. sinensis* will provide insights into the development of strategies against infections and for sustainable farming. Moreover, the public genomic sequences and transcriptomic data of *P. sinensis* [26–28] can provide valuable information for the characterization and functional exploration of TLR family genes in *P. sinensis*. Previous studies in *P. sinensis* have demonstrated the functional and expression analysis of a few PsTLRs [17,29]. However, the responses of the PsTLR family to microbial infection are not well clear, and the systematic knowledge of PsTLRs in *P. sinensis* is still lacking.

In this study, to systematically characterize the *TLR* family genes in *P. sinensis*, a whole genomic search and identification of *PsTLRs* were performed. The major aim of this study was to comprehensively analyse the structure feature and evolutionary relationship of PsTLR proteins and to detect the expression patterns of *PsTLR* genes under *A. hydrophila* challenge. A putative protein interaction network related to TLR signalling was also predicted in *P. sinensis*. The results of this study will provide more insights into the functional roles of PsTLRs in regulating immune responses and will contribute to the further elucidation of molecular mechanisms underlying innate immunity.

2. Materials and methods

2.1. Ethics statement

In this study, all experimental procedures and animal care were conducted according to the guidelines of the Animal Research Institute Committee (Northwest A&F University, Shaanxi, China). The protocol was approved by the Science and Technology Agency of Shaanxi Province under permit NO. SYXK (SN) 2018-0003, and all efforts were made to minimize animal suffering. The field studies did not involve any endangered or protected species.

2.2. Animals and bacterial infection

Healthy Chinese soft-shelled turtles (weighing approximately 1.0 kg, 3 years old) were obtained from Yangcheng Lake in Suzhou (31°N, 120°E), in the southeast of China. These turtles showed no clinical signs or laboratory evidence of *A. hydrophila* or other infections and were acclimated in the laboratory for one week before experiments. To analyse the tissue-specific expression of *TLR* mRNA in healthy animals, different tissue specimens, including heart, spleen, blood, liver, intestine and kidney, were collected from three healthy *P. sinensis* after anaesthesia with an intraperitoneal administration of sodium pentobarbital (20 mg/kg). Thirty *P. sinensis* specimens were divided equally into an infection group and a control group. *A. hydrophila* infection was performed as described previously [30]. In the infection group, each turtle was intraperitoneally challenged with live cells of *A. hydrophila* (10^6 CFU, strain AS 1.927, China General Microbiological Culture Collection Center, Beijing, China). In the control group, each animal received an equal volume of PBS intraperitoneally. Spleens were collected from three infected individuals and three control individuals at 6, 12, 24, 48 and 72 h post-infection and were immediately stored in liquid nitrogen until RNA extraction.

2.3. Identification of TLR family genes and sequence analysis

To identify *TLR* family genes in *P. sinensis*, the reported human and mouse TLR protein sequences were downloaded from NCBI database and were used as BLASTP queries to search against the genome protein sequences of *P. sinensis* [26]. Meanwhile, the TIR domain (Pfam PF01582; http://pfam.sanger.ac.uk) was also used to search against the genome protein sequences of *P. sinensis* using HMMER (Hidden Markov Model, HMM, version 3.2.1) search tool with an E-value cut-off 1.0. The obtained putative TLR gene sequences were confirmed and subjected to further analysis against the public databases, including the NCBI Conserved Domain Database (http://www.ncbi.nlm.nih.gov/cdd), SMART (http://smart.embl-heidelberg.de) and Pfam (http://pfam.xfam.org). The *TLR* gene candidates in *P. sinensis* were named as *PsTLRs* according to their homologous genes and annotations. Both the nucleotide and amino acid sequences of *PsTLR* genes were obtained. Genomic localization was analysed based on information from the *P. sinensis* genome and the NCBI database. The physiological and biochemical characteristics of PsTLR proteins, including their molecular weights, theoretical pI values, instability index, the aliphatic index and the grand average of hydropathicity (GRAVY), were analysed using the ProtParam tool of ExPASy (http://web.expasy.org/protparam). Only one common protein sequence from different transcripts of PsTLRs was selected for the following analysis. The conserved functional domains of PsTLR proteins were predicted through SMART online searching with default parameters.

2.4. Phylogenetic analysis and syntenic analysis of TLR family genes

Whole genome-wide searches of *TLR* family genes in 13 other species, including human (*Homo sapiens*), house mouse (*Mus musculus*), platypus (*Ornithorhynchus anatinus*), turkey (*Meleagris gallopavo*), chicken (*Gallus gallus*), American alligator (*Alligator mississippiensis*), green anole (*Anolis carolinensis*), western painted turtle (*Chrysemys picta*), three-toed box turtle (*Terrapene mexicana*), green sea turtle (*Chelonia mydas*), African clawed frog (*Xenopus laevis*), zebrafish (*Danio rerio*) and fruit fly (*Drosophila melanogaster*), were also performed, and these TLR protein sequences were downloaded and used for phylogenetic analysis. The information of the studied TLR proteins from the 13 species is listed in Supplementary Table S1. The phylogenetic relationships among *P. sinensis* and the 13 species were analysed using TimeTree server (http://www.timetree.org). The multiple alignments of TLR proteins were performed using DNAMAN 6.0 software with default parameters. A phylogenetic tree was constructed using MEGA

Table 1
The *PsTLR* family genes identified in *Pelodiscus sinensis*.

Name	Ensembl ID	NCBI ID	Location	Nucleotide ID	Protein ID	CDS status	Nucleotide length	Amino acid length
PsTLR1	ENSPSIG00000012620	102460455	NW_005856840	XM_006129518.3	XP_006129580.1	Complete	1965	654
PsTLR2-1	ENSPSIG00000000529	102457158	NW_005851767	XM_014574244.2	XP_014429730.1	Complete	2352	783
PsTLR2-2	–	102445063	NW_005854040	XM_014571663.2	XP_014427149.1	Complete	2592	863
PsTLR2-t2	ENSPSIG00000000537	102457570	NW_005851767	XM_025185305.1	XP_025041090.1	Complete	2352	783
PsTLR3	ENSPSIG00000010900	102456651	NW_005856643	XM_014576247.2	XP_014431733.1	Complete	2691	896
PsTLR4	ENSPSIG00000003827	102448887	NW_005854608	NM_001286933.1	NP_001273862.1	Complete	2502	833
PsTLR5	ENSPSIG00000000533	102460005	NW_005853122	XM_025180981.1	XP_025036766.1	Complete	2580	859
PsTLR7	ENSPSIG00000000409	102455967	NW_005855059	XM_014573459.2	XP_014428945.1	Complete	3153	1050
PsTLR8-1	ENSPSIG00000000427	102456214	NW_005855059	XM_006122845.3	XP_006122907.1	Complete	3078	1025
PsTLR8-2	ENSPSIG00000000439	102456470	NW_005855059	XM_014573452.2	XP_014428938.1	Complete	3078	1025
PsTLR8-3	ENSPSIG00000010094	102445423	NW_005855059	XM_006122794.3	XP_006122856.1	Complete	3138	1045
PsTLR9	ENSPSIG00000012812	102444127	NW_005854103	XM_014571799.2	XP_014427285.2	Complete	3273	1090
PsTLR10	–	102445089	NW_005856840	XM_025187956.1	XP_025043741.1	Complete	825	274
PsTLR13-1	ENSPSIG00000000250	102461996	NW_005871014	XM_006138146.3	XP_006138208.2	Complete	2865	954
PsTLR13-2	–	102451718	NW_005871014	XM_006138102.3	XP_006138164.2	Complete	2865	954

7.0 [31] with the neighbourhood-joining (NJ) method and bootstrap values of 1000 replicates. Different subfamilies by classification were named according to the previous reports. Syntenic analysis was carried out by searching the syntenic regions surrounding the TLR proteins based on NCBI database. The neighbouring genes were also identified and compared among *P. sinensis*, *H. sapiens*, *C. picta* and *T. mexicana*.

2.5. Interaction relationships and functional enrichments of PsTLR proteins

The putative protein interactions were predicted based on the PsTLR protein sequences by using the online STRING software (http://string-db.org). The interaction relationships were analysed according to the information from the *P. sinensis* genome. The interacting partners of PsTLR proteins were also identified. The predicted networks were generated by setting the minimum required interaction score ≥0.7. Functional enrichment and annotation analysis were performed based on the Kyoto Encyclopaedia of Genes and Genomes (KEGG, http://www.kegg.jp/kegg/pathway.html) database with a *P*-value ≤ 0.05.

2.6. Protein structure analysis and binding site prediction

The protein sequences of TLR genes were used to predict the 3D protein structures. Homology models of TLR proteins were prepared with the Phyre2 server [32]. Secondary structure prediction and domain analyses were also performed. The known structures of homologue proteins from human and mouse were used as templates. The prediction of the binding sites was performed by the 3DLigandSite server [33]. PyMOL Viewer software was used to view the 3D structures and to perform structural comparisons.

2.7. Expression analysis by quantitative real-time PCR

Total RNA was extracted using TRIzol reagent (Invitrogen, Carlsbad, CA, USA) according to the manufacturer's protocol and was reverse transcribed into cDNA using the SuperScript First-Strand Synthesis System (Invitrogen, Carlsbad, CA, USA). Quantitative real-time PCR (qRT-PCR) analysis was performed to validate the expression patterns of *PsTLR* genes using SYBR® Premix Ex Taq™ II (TaKaRa, Dalian, China) on a BioRad iQ5 real-time PCR platform (BioRad, USA) according to the previously reported methods [27,28]. Briefly, each reaction was performed in a total volume of 20 μL containing 10 μL SYBR green reaction mix, 2.0 μL diluted cDNA template and 0.8 μL each primer using the following PCR program: 95 °C for 3 min, and 40 cycles by 95 °C for 30 s, 58 °C for 30 s and 72 °C for 30 s. Melting curves were obtained to verify the amplification specificity through a stepwise heating of the amplicon from 60 to 95 °C. Specific primers were designed using Beacon Designer software (Premier Biosoft International, USA) and are listed in Supplementary Table S2. Three biological replicates and three technological replicates were employed. The *β*-Actin gene was used as a reference gene to normalize the gene expression levels. Relative expression levels of genes were calculated using the $2^{-\Delta\Delta CT}$ method [34]. Java Treeview software [35] was employed to generate the heat maps of gene expression levels by using the values of $\log_2$ fold change (expression in infection group/expression in control group).

2.8. Statistical analysis

The data were presented as the means ± SEM. Statistical analysis was conducted with SPSS 16.0 software (Inc., Chicago, IL, USA), and significance was assessed by one-way ANOVA. A *P*-value < 0.05 was considered statistically significant.

3. Results

3.1. Identification of PsTLR family genes in the Chinese soft-shelled turtle

In this study, genome-wide analysis of *TLR* family genes was performed by searching against the *P. sinensis* genome sequences. The obtained sequences of candidate *TLR* genes were further verified through the public NCBI, SMART and Pfam databases. Ultimately, 15 TLR genes were identified and named *PsTLR1-13* (Table 1). Several genes such as *PsTLR1*, *PsTLR2-1*, *PsTLR3*, *PsTLR5* and *PsTLR8-3*, had multiple transcripts. These identified genes contained the full-length coding sequences. Among these *PsTLR* family genes with the exception of *PsTLR10*, *PsTLR1* had the minimum lengths of nucleotide (1,965) and amino acid sequences (654), whereas *PsTLR9* had the maximum lengths of nucleotide (3,273) and amino acid sequences (1,090). Physiological and biochemical properties analyses of PsTLR proteins (except PsTLR10) showed that their molecular weights ranged from 76.00 (PsTLR1) to 122.26 kDa (PsTLR9), and their theoretical pI values ranged from 6.01 (PsTLR8-3) to 8.93 (PsTLR8-2). More detailed information, including gene ID, nucleotide and amino acid sequences, genomic location, instability index, aliphatic index and GRAVY, for these *PsTLR* genes is listed in Supplementary Table S3.

To better understand the characteristics of PsTLR proteins, a phylogenetic analysis was carried out based on their full-length amino acid sequences (Fig. 1A). Furthermore, the conserved functional domains of the 15 PsTLR proteins were predicted by SMART analysis. The results showed that these PsTLR proteins shared typical functional domains, such as the TIR domain, the LRR domain and the transmembrane region (Fig. 1C). Moreover, the number of LRR motifs varied among these PsTLR proteins (Fig. 1B). The majority of PsTLR proteins had more than eight LRR motifs, except PsTLR1 and PsTLR10. In addition, the TIR domain and transmembrane region were not found in the PsTLR10

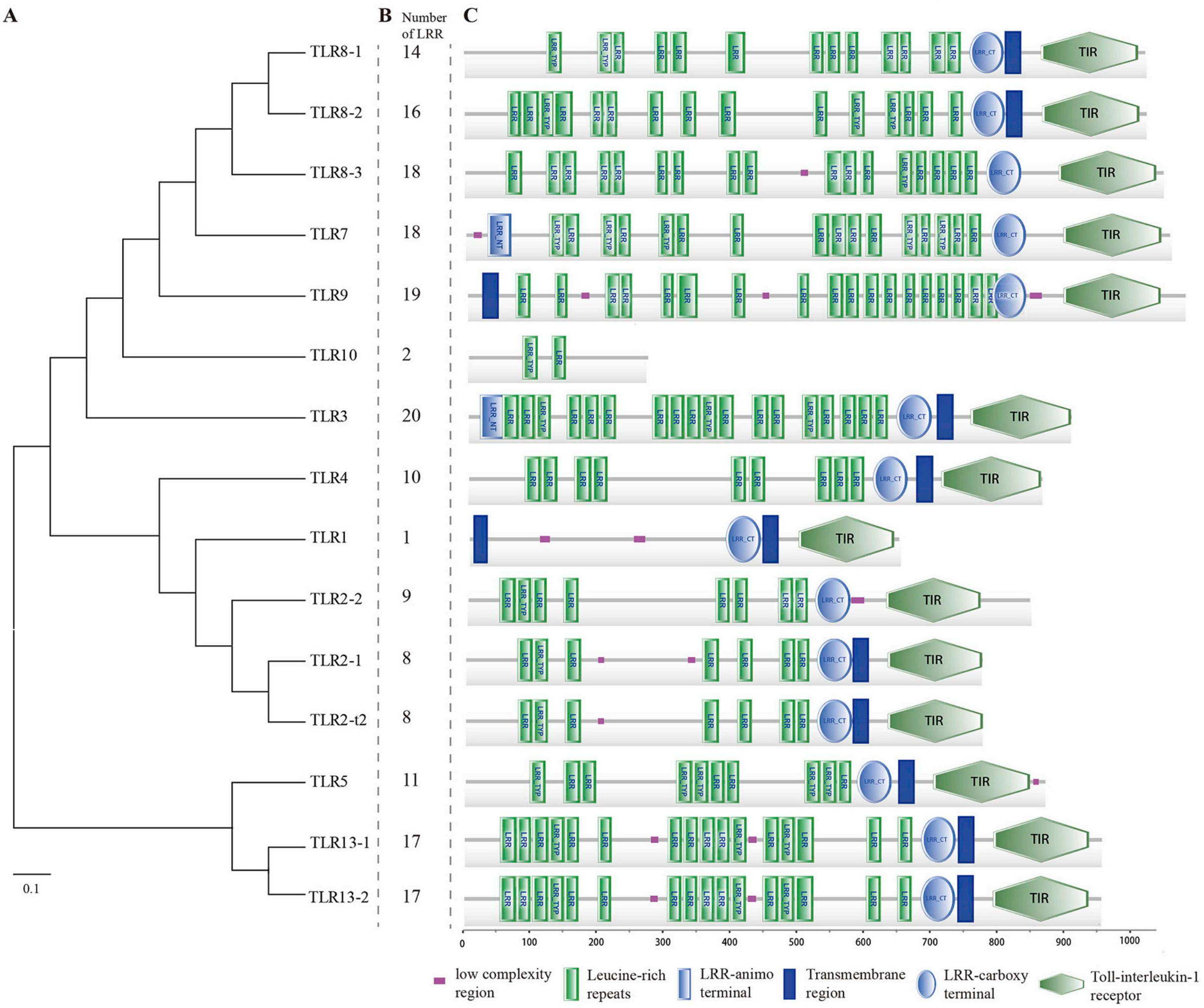

Fig. 1. Comparison analysis among the identified PsTLRs in *Pelodiscus sinensis*. A: Phylogenetic relationships among 15 PsTLR proteins. B: The number of LRR domains in PsTLRs. C: The conserved domains of PsTLR proteins.

protein, which only included two LRR domains.

3.2. Phylogenetic analysis and classification of TLR family genes

To investigate the phylogenetic relationship and comparative evolution of *TLR* genes among various species, the *TLR* family genes from 13 other species were searched and collected from their genome sequences and the NCBI database (Fig. 2). Comparative analysis showed that the number of *TLR* family members was diverse in different species. Analysis of the genetic evolution of species indicated that *P. sinensis* had the closest relationships with green sea turtle (*Chelonia mydas*), western painted turtle (*Chrysemys picta*) and three-toed box turtle (*Terrapene mexicana*), and all four species belonged to the cryptodira branch (Fig. 2). Notably, the *TLR* family members in *P. sinensis*, as well as the number of *TLR* genes, were very similar to those in *C. mydas*, *C. picta* and *T. mexicana*, in agreement with the evolutionary relationships among the four species. Moreover, a total of 179 TLR homologue proteins from *P. sinensis* (15 sequences) and 13 other species (164 sequences) were subjected to phylogenetic analysis. A phylogenetic tree was constructed using the NJ method (Fig. 3). These TLR homologs were classified into six subfamilies, including the TLR1, TLR3, TLR4, TLR5, TLR7 and TLR11 subfamilies. The greatest number of genes was assigned to the TLR1 subfamily, followed by the TLR7 and TLR11 subfamilies. Additionally, all of the PsTLR proteins shared the closest evolutionary relationship with the corresponding proteins from *C. mydas*, *C. picta* and *T. mexicana* (shown in red lines in Fig. 3). In general, the results suggested the evolutionary conservation of TLR homologous proteins among various species.

3.3. Localization and syntenic analysis of PsTLR genes

In this study, genomic localization showed that the 15 *PsTLR* genes were distributed across nine different scaffolds in the *P. sinensis* genomes (Supplementary Table S3). Several pairs of *PsTLR* genes were located in the same scaffold, including *PsTLR7* and *PsTLR8* anchoring on NW_005855059, and *PsTLR1* and *PsTLR10* anchoring on NW_005856840 (Fig. 4). Moreover, some duplicated genes were also arranged on the same scaffold, including *PsTLR2-t2/PsTLR2-1* (NW_005851767), *PsTLR8-1/PsTLR8-2/PsTLR8-3* (NW_005855059), and *PsTLR13-1/PsTLR13-2* (NW_005871014). To further examine the gene localization and to confirm the identities of *PsTLR* genes, the neighbouring genes of *PsTLRs* and their homologs from *H. sapiens*, *C. picta* and *T. mexicana* were searched, and the synteny analyses were performed based on their genomic information and the NCBI database. *H. sapiens* represents the reference species, and *C. picta* and *T. mexicana* represent species close to *P. sinensis* in evolution. The comparative analysis of gene organization showed that the up- and down-stream genes surrounding the *TLRs* were highly conserved among *P. sinensis*, *H. sapiens*, *C. picta* and *T. mexicana*. Furthermore, the duplicated *PsTLR2*, *PsTLR8* and *PsTLR13* homologs were near each other and were

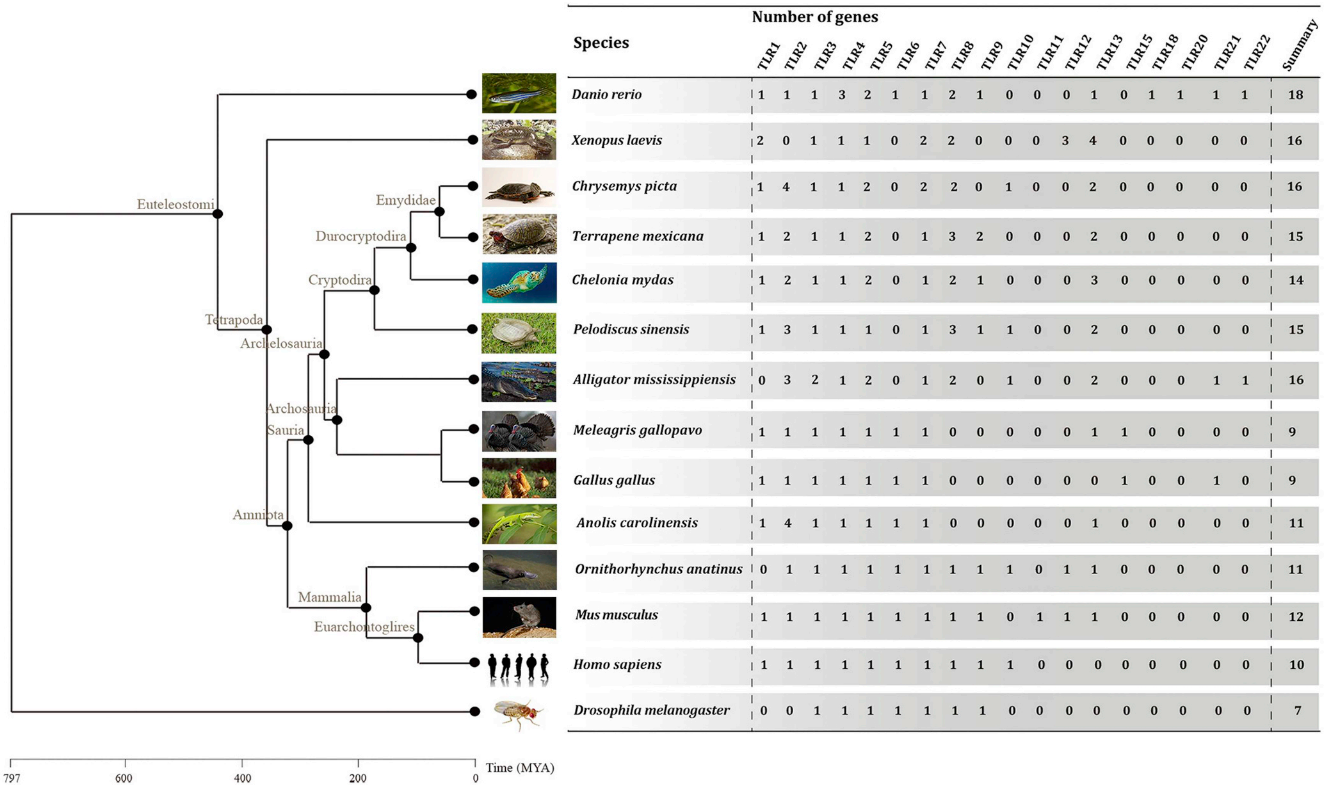

Species	TLR1	TLR2	TLR3	TLR4	TLR5	TLR6	TLR7	TLR8	TLR9	TLR10	TLR11	TLR12	TLR13	TLR15	TLR18	TLR20	TLR21	TLR22	Summary
	Number of genes																		
Danio rerio	1	1	1	3	2	1	1	2	1	0	0	0	1	0	1	1	1	1	18
Xenopus laevis	2	0	1	1	1	0	2	2	0	0	0	3	4	0	0	0	0	0	16
Chrysemys picta	1	4	1	1	2	0	2	2	0	1	0	0	2	0	0	0	0	0	16
Terrapene mexicana	1	2	1	1	2	0	1	3	2	0	0	0	2	0	0	0	0	0	15
Chelonia mydas	1	2	1	1	2	0	1	2	1	0	0	0	3	0	0	0	0	0	14
Pelodiscus sinensis	1	3	1	1	1	0	1	3	1	1	0	0	2	0	0	0	0	0	15
Alligator mississippiensis	0	3	2	1	2	0	1	2	0	1	0	0	2	0	0	0	1	1	16
Meleagris gallopavo	1	1	1	1	1	1	1	0	0	0	0	0	1	1	0	0	0	0	9
Gallus gallus	1	1	1	1	1	1	1	0	0	0	0	0	0	1	0	0	1	0	9
Anolis carolinensis	1	4	1	1	1	1	1	0	0	0	0	0	1	0	0	0	0	0	11
Ornithorhynchus anatinus	0	1	1	1	1	1	1	1	1	1	0	1	1	0	0	0	0	0	11
Mus musculus	1	1	1	1	1	1	1	1	1	0	1	1	1	0	0	0	0	0	12
Homo sapiens	1	1	1	1	1	1	1	1	1	1	0	0	0	0	0	0	0	0	10
Drosophila melanogaster	0	0	1	1	1	1	1	1	1	0	0	0	0	0	0	0	0	0	7

Fig. 2. Statistics of *TLR* family genes in *Pelodiscus sinensis* and 13 other species. MYA: million years ago.

tandemly organized on the scaffolds (Fig. 4). The homologs of *PsTLR7* and *PsTLR8* in *H. sapiens*, *C. picta* and *T. mexicana* also shared the neighboured positions (Fig. 4C), as well as the homologs of *PsTLR1* and *PsTLR10* in *H. sapiens* and *C. picta* (Fig. 4A). Importantly, three duplicated genes of *TLR8* were found in *P. sinensis* and *T. mexicana*, whereas only two and one *TLR8* were searched in *H. sapiens* and *C. picta*, respectively. Similarly, two duplicated *TLR2* genes were found in *P. sinensis* and *C. picta*, while only one was found in *H. sapiens* and *T. mexicana*. In addition, the *TLR6* gene in human (Chr4) was not found in *P. sinensis* and *C. picta*. These results will provide insights into the evolution of *TLR* orthologous genes in different species.

3.4. Interaction analysis of PsTLR proteins

The putative interaction network of PsTLR proteins in *P. sinensis* was predicted by using the online STRING server. A total of 20 proteins, including ten PsTLR proteins and ten functional partner proteins (such as PsMyD88, PsTRAF6 and PsIKBKG) were identified in the interaction network (Supplementary Table S4; Fig. 5). Functional annotations and enrichment analysis revealed that all the functional partners in the network were involved in TLR-related signalling pathways. Almost all the proteins (except PsUBE2N and PsBIRC2) participated in the Toll-like receptor signalling pathway (KEGG ID 4620; Supplementary Table S4). Furthermore, PsTRAF6, PsIKBKG and PsMAP3K7 were involved in the ‘MAPK signalling pathway’ (KEGG ID 4010), and PsMyD88 and PsIKBKG were involved in the ‘Apoptosis pathway’ (KEGG ID 4210). Protein-protein associations revealed that all ten PsTLR proteins had interaction relationships with the PsMyD88 protein (Fig. 5). Moreover, the PsMyD88 protein, located in the central node of the network, was found to harbour 16 interacting proteins, followed by the PsTRAF6 protein with 14 interacting proteins, implying that PsMyD88 and PsTRAF6 may play key roles in TLR signalling. In addition, PsMyD88, PsTOLLIP and PsTIRAP were predicted to be the neighbourhood genes, and PsTLR2-1 and PsTLR2-t2 having the known interactions were homologous proteins. Taken together, these protein interaction predictions and the results of the functional enrichment analysis will contribute to the further exploration of PsTLR functions.

3.5. Expression patterns of PsTLRs in different tissues of P. sinensis

To validate the tissue-specific expression patterns of *PsTLR* genes, qRT-PCR analysis was performed to detect the relative expression levels of *PsTLRs* in different healthy tissues of *P. sinensis*, including heart, spleen, blood, liver, intestine and kidney. Except for *PsTLR10*, with an incomplete organization of the conserved domains for TLR protein, 13 *PsTLR* genes were selected for expression analysis, among which *PsTLR13* was used to represent *PsTLR13-1* and *PsTLR13-2* genes with the same sequences. The results showed that these *PsTLR* genes were constitutively expressed in six tissues of *P. sinensis* (Fig. 6). Moreover, the expression levels of *PsTLRs* varied among six different tissues. Highest expression levels of *PsTLR2-1*, *PsTLR4* and *PsTLR13* were found in the spleen, and with the second-highest levels in the blood. Specifically, *PsTLR2-1* and *PsTLR4* were expressed at significantly higher levels in the spleen. Higher expression levels of *PsTLR2-2*, *PsTLR5*, *PsTLR7*, *PsTLR8-1* and *PsTLR8-3* were detected in the blood. *PsTLR1* and *PsTLR2-t2* were highly expressed in the liver, and *PsTLR3*, *PsTLR8-2* and *PsTLR9* were highly expressed in the intestine. In addition, most of these *PsTLR* genes had lower expression levels in the heart and kidney.

3.6. Expression of PsTLR and its downstream genes after A. hydrophila infection

To further reveal the putative biological roles of *PsTLR* genes, their expression patterns in *P. sinensis* spleen were detected at 6, 12, 24, 48 and 72 h after *A. hydrophila* infection. The relative expression levels of *PsTLRs* were examined by qRT-PCR analysis, and heat maps of the expression patterns were generated. The results showed that all the *PsTLR* genes were differentially expressed under treatment in comparison with the control group (Supplementary Table S5; Fig. 7). Most *PsTLRs* exhibited up-regulated expressions at different time points post-infection,

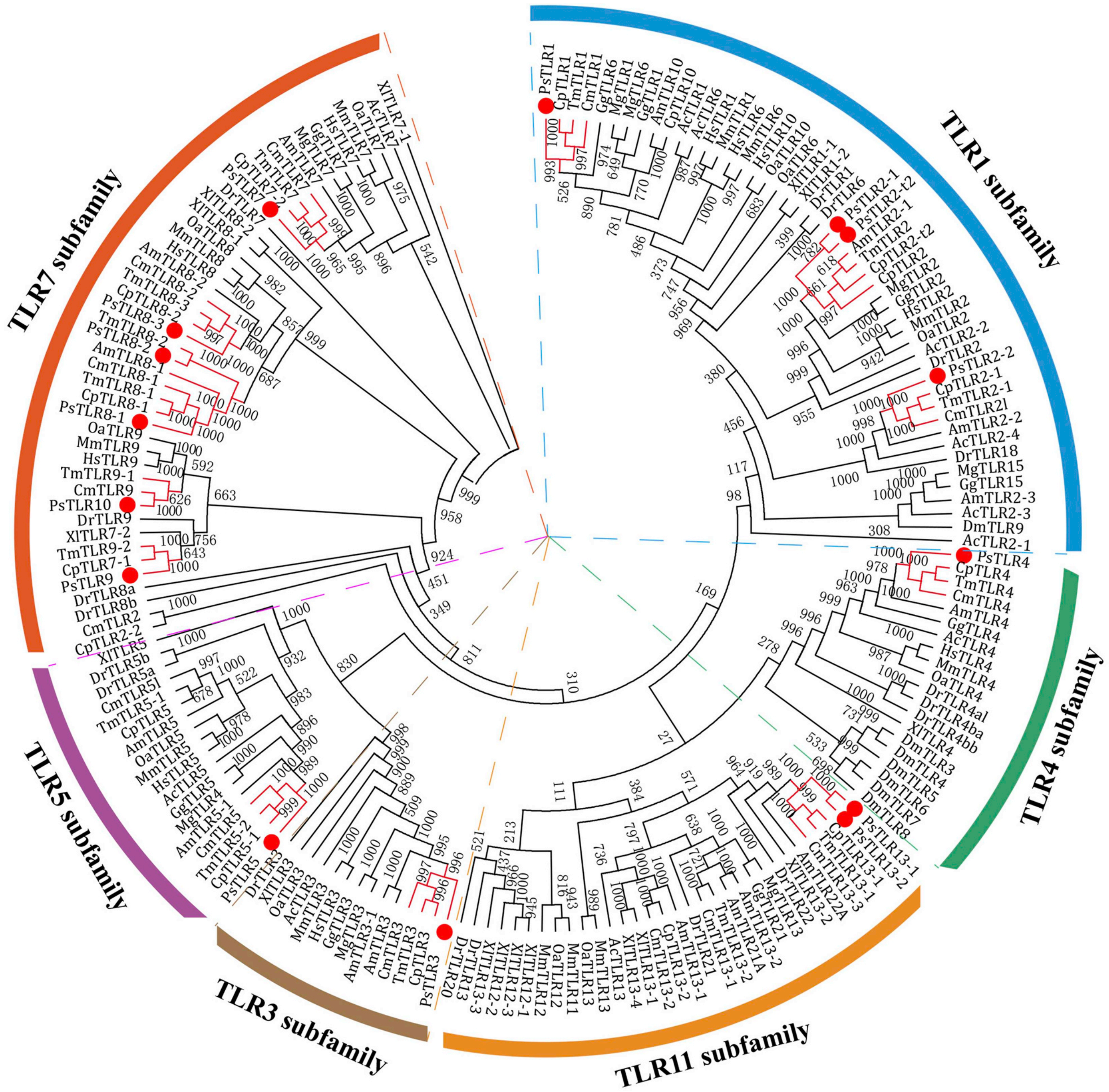

Fig. 3. Phylogenetic analysis and classification of TLR homologs from *Pelodiscus sinensis* and 13 other species. Red circles mark the PsTLR proteins in *Pelodiscus sinensis*. Red lines represent the close relationships between PsTLRs and the corresponding homologs. (For interpretation of the references to colour in this figure legend, the reader is referred to the Web version of this article.)

whereas *PsTLR2-2* and *PsTLR2-t2* were down-regulated at 36 and 72 h, respectively. Notably, *PsTLR2-1* and *PsTLR4* genes displayed significantly up-regulated expressions after *A. hydrophila* infection. The expression level of the *PsTLR2-1* gene increased rapidly at 6 h and reached a peak at 12 h after infection, with a subsequent gradual decrease until 72 h post-infection (Fig. 8). Along with the stimulation of *A. hydrophila*, peak expression of the *PsTLR4* gene was detected at 6 h post-infection, after which its expression level declined. The rapid responses of the *PsTLR2-1* and *PsTLR4* genes to *A. hydrophila* infection may be associated with their roles in regulating the immune response.

In the TLR signalling pathway, TLRs can activate downstream targets (such as MyD88) and immune-related factors (such as TNF, IL1β and IL6) in response to environmental stress [2,36]. In the present study, the *PsMyD88* (NM_001286912.1), *PsTNF* (XM_014575959), *PsIL1β* (NM_001317048) and *PsIL6* (XM_006138351) genes were also selected for expression analysis. The results suggested that the expression levels of the four detected genes were generally elevated in the spleen of *P. sinensis* upon *A. hydrophila* infection (Fig. 8). Rapid increases in *PsMyD88* and *PsIL1β* expression levels were detected at 12 h after infection, in agreement with the expression variations of the *PsTLR2-1* and *PsTLR4* genes during the initial stage of infection. Furthermore, *PsIL1β* and *PsIL6* genes were steadily up-regulated at different time points after infection. In addition, *PsMyD88* had a transient lower expression level at 24 h, and the *PsTNF* level decreased lightly at 72 h post-infection. The results indicated that the downstream genes of TLRs and the major inflammatory factors can sense the signals from TLRs and are involved in the immune response in *P. sinensis* [1,36].

3.7. Protein structure analysis and binding site prediction

To explore the potential functions of PsTLR2-1 and PsTLR4 proteins, their protein structures were predicted and built by the homology modelling method. Secondary structure analysis showed that PsTLR2-1 was mainly composed of 24% alpha-helix and 13% beta-strand, and

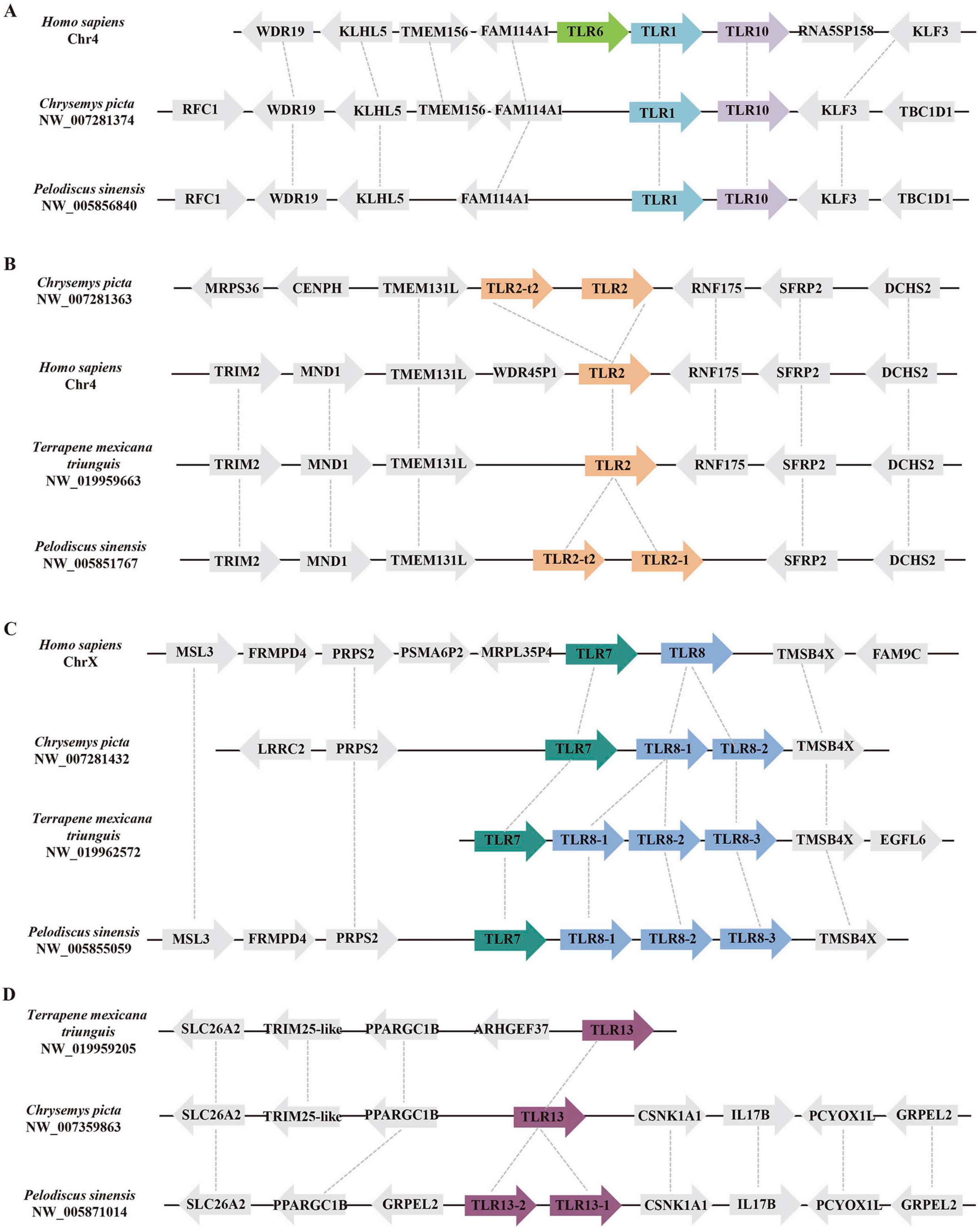

Fig. 4. Syntenic analysis of the selected *TLRs* and the neighbouring genes among *Pelodiscus sinensis*, *Homo sapiens*, *Chrysemys picta* and *Terrapene mexicana*.

PsTLR4 mainly consisted of 25% alpha-helix and 13% beta-strand (Supplementary Table S6). As a result, the 3D structures of both PsTLR2-1 and PsTLR4, which harbour multiple LRR domains, exhibited horseshoe shapes (Fig. 9A, D). Moreover, the potential binding sites in the PsTLR2-1 and PsTLR4 proteins were predicted by the 3DLigandSite server and were marked in blue (Fig. 9B, E). Ten binding sites (including 391 PHE, 408 LEU, 409 SER, 410 HIS, 411 LEU, 412 LYS, 413 HIS, 414 LEU, 415 THR and 416 HIS) were found in PsTLR2-1 protein, and nine binding sites (including 376 GLU, 377 LYS, 378 PHE, 399 CYS, 401 ASP, 402 SER, 417 PHE, 418 ASN and 438 ARG) were identified in the PsTLR4 protein. Furthermore, to verify the predicted protein structures, the 3D structures of TLR2 and TLR4 homologue proteins from human (*H. sapiens*), mouse (*M. musculus*) and chicken (*G. gallus*) were also analysed and aligned with PsTLR2-1 and PsTLR4 proteins.

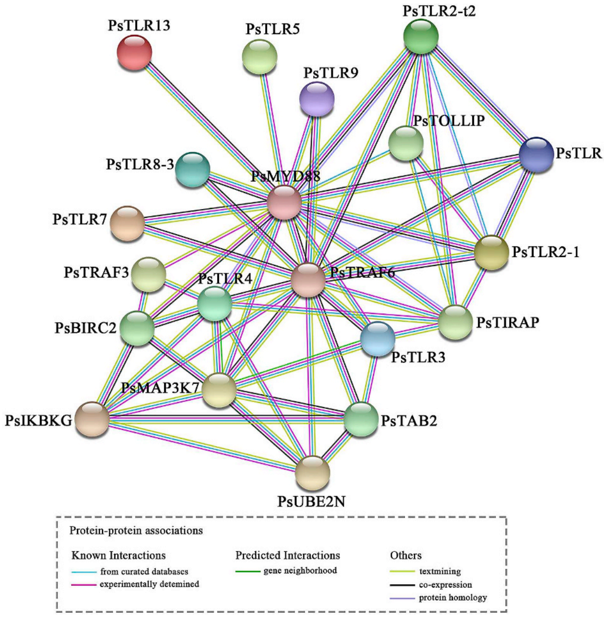

Fig. 5. Putative interaction network of PsTLR proteins in *Pelodiscus sinensis*.

The homology models were generated using the human TLR2 (c5d3iA) and TLR4 (c3fxiA) templates. As shown in Fig. 9C, the protein structures among the PsTLR2-1, HsTLR2, MmTLR2 and GgTLR2-1 proteins almost completely overlapped. In addition, PsTLR4 had a similar structure compared to HsTLR4, MmTLR4 and GgTLR4, except that PsTLR4 had one more helix located in amino acids 361-368 (Fig. 9F). These observations further indicated the high conservation of TLR proteins among different species, which coincides with the results of the phylogenetic analysis.

4. Discussion

Toll-like receptors (TLRs) have evolved prominent roles in initiating immune responses to infection and are key sentinels of the innate immune system [2,4]. Recognizing a wide range of highly conserved PAMPs enables TLRs to trigger the activation of signalling cascades and to regulate the immune mechanisms [3,4]. The basic architecture of TLRs consisting of the extracellular LRR domains are responsible for PAMP recognition and transmit the signals through TIR-containing intracellular adapter proteins to cause inflammatory responses [5,37,38]. TLRs are generally conserved throughout evolution and are the most widespread among vertebrates [5,10]. A series of TLR family genes and an increasing number of target genes have been identified in many species. To date, genomic analyses have identified 28 TLR repertoires across different vertebrate species, where mammals display TLR1-13 and fishes also display TLR14-28 [11,39,40]. Although TLRs have been extensively studied in various species and are reported to play fundamental roles in the immune response, little knowledge of the comprehensive identification and functional exploration of *P. sinensis* TLRs was previously available. In this study, genome-wide analysis identified 15 TLR genes representing *PsTLR1-13* in *P. sinensis*, and complete sequences were achieved for nearly all the *PsTLRs*. Moreover, the protein structures, expression characteristics and evolution of *PsTLR* family genes were explored in the present study, which will contribute to the further understanding of the putative roles of *PsTLRs* and to achieving a comprehensive overview in *P. sinensis*.

It is believed that the evolutionarily conserved protein structures of TLRs are usually required for their functional roles in regulating the innate immune system [1,41]. Previous studies on comparisons of protein structures in TLRs have indicated that their typical secondary structures were conserved among various TLRs [5,42,43]. Our studies revealed that the PsTLRs contained the conserved functional domains including the TIR domain, various LRR domains and the transmembrane region. The results meet the specific features of TLR proteins [5,38,43] and verify the reliability of the identified PsTLRs in *P. sinensis.* Contrary to the single TIR domain across PsTLR family members, the number and position of LRR domains varied among PsTLRs. LRR domains are involved in pathogen recognition, and the divergence in domain number may affect the ligand-binding specificities and determine the function diversity of PsTLRs [5,37,41]. Moreover, the similar arrangement of conserved domains in PsTLR proteins indicated their close phylogenetic relationships. The phylogeny and classification of TLRs from *P. sinensis* and 13 other species suggested that the TLR homologs were assigned into six major classes, including the TLR1, TLR3, TLR4, TLR5, TLR7 and TLR11 subfamilies. Similar classifications and phylogenies of TLRs have been reported in Yesso scallop, common carp and Tibetan fish [42–44], revealing that TLR proteins are highly conserved among different species [10]. Most PsTLRs were found to be close to the homologs from *C. mydas*, *C. picta* and *T. mexicana* by phylogenetic analysis, which was consistent with the evolutionary relationships among these turtle species. These results imply that the near relationships in the evolution of species seem to allow high similarities in TLR homologs.

The high diversity in the number of TLR family genes is accompanied by the evolutionary and genome duplication events in species [10,41]. Genome duplication is essential for generating the duplicated genes or novel genes with divergent functions [45,46]. It has been reported that vertebrates underwent two rounds of large-scale gene duplication early their evolution [47]. More copies of TLRs have been identified in some vertebrates, especially in fish species [40,43,44,48]. In *P. sinensis*, duplicated gene pairs of *PsTLR2*, *PsTLR8* and *PsTLR13* were found, with these duplicated genes neighbouring each other on the same scaffold. Compared to lower-level fish in evolution, fewer and unequal numbers of gene duplications were generated in *P. sinensis*; hence, we speculated that the duplicated genes may occur from small-scale copies of chromosomal sections or individual genes [47]. Concurrent with gene duplication, gene loss is also an important evolutionary process for gene family formation and species evolution [46]. In the present study, *TLR6* was found in the human genome, located on the Chr4 of *H. sapiens*, whereas the homologous *PsTLR6* was not found in *P. sinensis*. Actually, the *TLR6* homologue genes were found to be homologous to *TLR1* in chicken and cattle [49,50]. The absent *PsTLR6* gene in the genome of *P. sinensis* may owe to the individual gene loss event. Previous analysis on the neighbouring genes around *TLR4* showed that *PsTLR4* was orthologous to the *TLR4* genes from human and chicken [17]. In this study, syntenic analysis of genes surrounding *TLRs* was performed against the genomes of *P. sinensis*, *H. sapiens*, *C. picta* and *T. mexicana*. As a result, the gene organization and arrangement of *TLR* homologs, including the neighbouring and duplicated genes, were parallel among *P. sinensis*, *H. sapiens*, *C. picta* and *T. mexicana*, further indicating that *TLR* genes were highly conserved in the evolution. Moreover, the most similar tandem organizations of genes among *P. sinensis*, *C. picta* and *T. mexicana* were detected, demonstrating the close evolutionary relationships among these turtles.

TLR-mediated immune responses appear to be involved in environmental adaptation [2,25]. The unnaturally high rearing density and the increase in infectious diseases seriously endanger the culture industry of aquatic animals [21,22]. The microbial diseases caused by bacteria have become one of the most serious threats to *P. sinensis*. It is widely reported that the increasing numbers of infectious diseases are found in *P. sinensis*, especially infection by *A. hydrophila*, one of the most frequently occurring pathogens [22–24]. In view of the roles of TLRs in detecting the microbial components and activating defensive

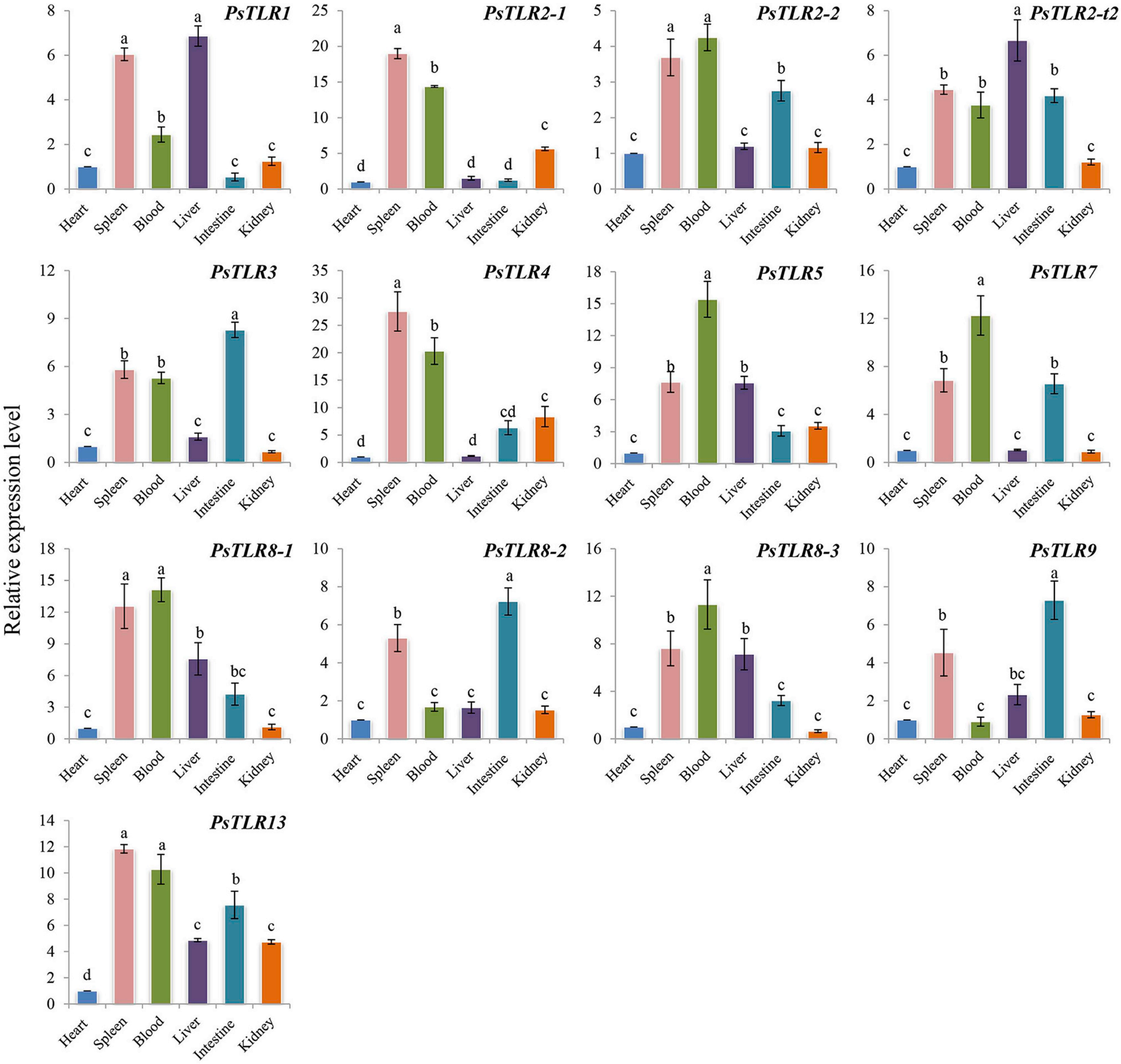

Fig. 6. Tissue-specific expressions of *PsTLR* genes in six different tissues (heart, spleen, blood, liver, intestine and kidney) of *Pelodiscus sinensis*. The value with a different letter indicates a significant difference at $P < 0.05$. Each bar shows the mean ± SEM of triplicate assays.

reactions, a better understanding of gene expressions of TLRs and the relevant signal factors upon bacterial challenge is very important undoubtedly. In this study, tissue-specific expression analysis of *PsTLR* genes showed that 13 selected *PsTLRs* exhibited constitutive expression in six different tissues of *P. sinensis*, suggesting the putative roles of *PsTLRs* in maintaining organismic homeostasis [43]. Notably, higher expression levels of several *PsTLRs* (especially *PsTLR2-1* and *PsTLR4*) were detected in the spleen, which is one of the major immune organs, indicating the participation of *PsTLRs* in the immune response and in agreement with previous reports [43,51]. Furthermore, the dynamic expression levels of these *PsTLRs* in the spleen of *P. sinensis* showed their differential expression patterns at different time points after *A. hydrophila* infection, which demonstrated the strong sensitivity of *PsTLRs* towards bacterial infection [25]. More importantly, consistent with previous studies [17,43,51], the significant increases in expression levels of *PsTLR2-1* and *PsTLR4* were detected at 12 h post-infection in the present study. The changes in *TLR2* and *TLR4* mRNA levels may suggest their functional roles upon stress challenge. As the important players in immunity, TLR2 and TLR4 have been reported to recognize the conserved components of Gram-negative bacteria including *A. hydrophila* [17,52]. Qi et al. [53] found significantly differential expression of *TLR2* following *A. hydrophila* infection in the Chinese giant salamander. In addition, Gong et al. [43] reported that carp *TLR4* can be induced after challenging with *A. hydrophila*. To further assess the potential biological roles of PsTLR2-1 and PsTLR4 in *P. sinensis*, the protein 3D structures were predicted and aligned to their homologs in human, mouse and chicken, which are higher-level species to *P. sinensis* in evolution. As expected, similar crystal structures of TLR2 and TLR4 proteins among these four species were obtained by structural comparison, implying that the putative roles of PsTLR2-1 and PsTLR4 may

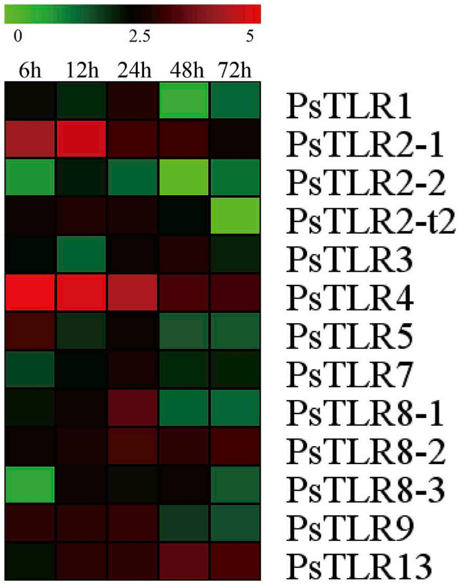

Fig. 7. Heat map of *PsTLR* gene expression levels in the spleen at different time points (6, 12, 24, 48 and 72 h) under *Aeromonas hydrophila* infection.

be similar to those of the orthologue proteins from human, mouse and chicken. Determining the protein functions of PsTLRs will require more in-depth studies in the further.

Series of TLRs and functional components have been implicated in the complex TLR signalling network [36]. The associations between TLRs and their downstream appropriate adaptor proteins are crucial for initiating inflammatory responses and manipulating immune homeostasis [1,3,36]. Intracellular MyD88 is an important adaptor protein that senses the signals from TLRs and dominates the MyD88-dependent pathway of TLR signalling pathway [30,38]. MyD88-mediated signalling cascades involve multiple signalling molecules, such as TIR domain containing adaptor protein (TIRAP), Toll interacting protein (TOLLIP), IL-1R-associated kinases (IRAKs), TAK1-binding protein 1 (TAB1) and TNF receptor-associated factor 6 (TRAF6), leading to TLR-induced signalling transduction [2,36]. In this study, several components participating in the TLR signalling pathway were detected by protein interaction analysis in *P. sinensis*, which included not only ten PsTLRs but also ten functional partner proteins, such as PsMyD88, PsTIRAP, PsTOLLIP, and others. The proposed interaction network will serve to improve the understanding of PsTLRs and the TLR signalling pathways in *P. sinensis*. Our previous study found that the differential expressions of *PsTLRs*, *PsMyD88* and some immune-related genes modulated the immune response and contributed to long-term sperm storage in female *P. sinensis* [27]. In the current study, upon *A. hydrophila* challenge, the *PsMyD88* gene expression level increased in *P. sinensis* spleen. Furthermore, three immune factors, *PsIL1β*, *PsIL6* and *PsTNF*, the downstream genes of the MyD88-dependent pathway, also exhibited significantly up-regulated expression patterns in the spleen after *A. hydrophila* infection. The induction of inflammatory cytokines requires the MyD88-activated TLR cascade [1,30,36]. Therefore, the expression variations of *PsTLRs* may mediate the MyD88-dependent pathway and then affect the levels of immune factors such as PsIL1β, PsIL6 and PsTNF, which directly initiates the immune responses in *P. sinensis*. Taken together, these observations reveal the potential pathway of TLR-MyD88-immune reaction signalling transduction in *P. sinensis*.

5. Conclusion

In this study, whole genome searches identified 15 candidate *PsTLR* family genes in *P. sinensis*, and complete sequences were obtained for all *PsTLR* genes. The conserved domain analysis revealed that PsTLR protein structures were highly conserved and consisted of a TIR domain, various LRR domains and a transmembrane region. Phylogenetic relationship and syntenic analyses indicated the evolutionary conservation of TLRs among 14 different species. Moreover, the proposed interaction network underlying the TLR signalling pathway provided rich information for PsTLR protein functions. Expression analysis revealed that the expression patterns of *PsTLR* genes were diverse in six different tissues of *P. sinensis*. Remarkably, the expression levels of *PsTLR2-1* and *PsTLR4* genes were highest in the spleen of *P. sinensis* and significantly increased upon *A. hydrophila* infection. *PsMyD88*, *PsIL1β*, *PsIL6* and

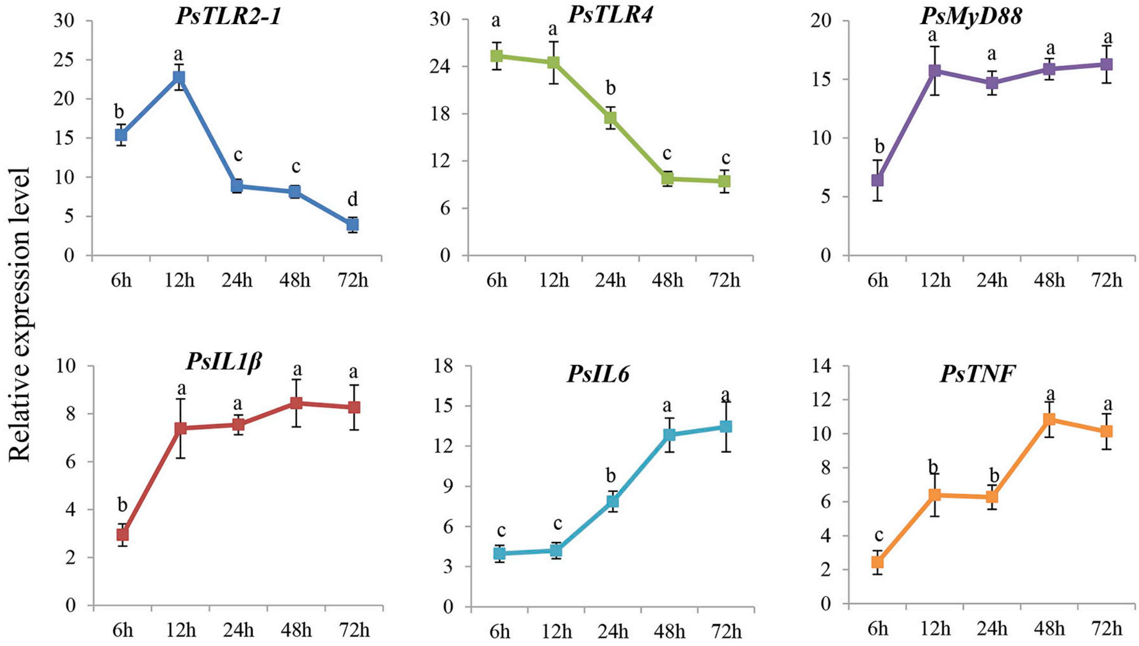

Fig. 8. Expression profiling of *PsTLR2-1*, *PsTLR4*, *PsMyD88*, *PsIL1β*, *PsIL6* and *PsTNF* genes in *Pelodiscus sinensis* spleen at 6, 12, 24, 48 and 72 h under *Aeromonas hydrophila* infection. The value with a different letter indicates a significant difference at $P < 0.05$. Each bar shows the mean ± SEM of triplicate assays.

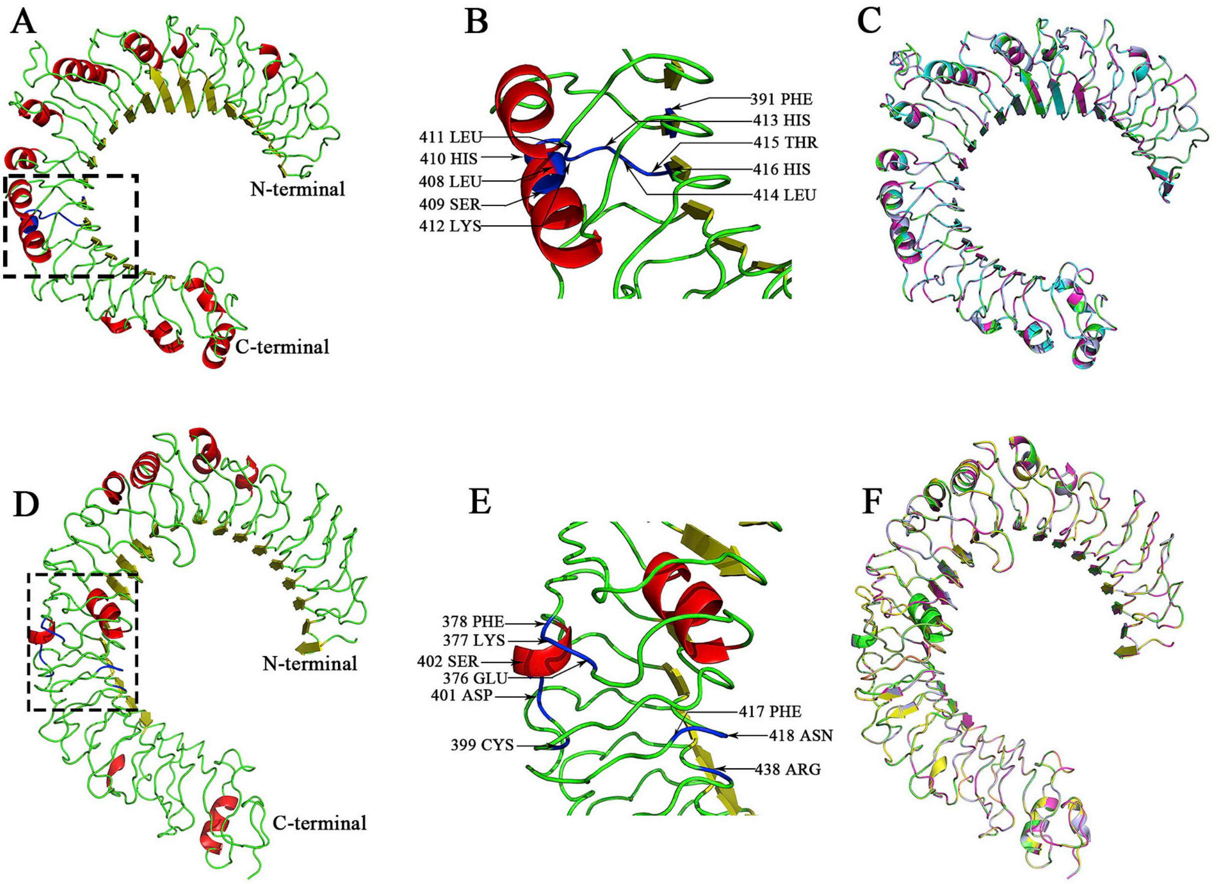

Fig. 9. TLR protein structure analysis. A, D: The predicted 3D protein structures of PsTLR2-1 and PsTLR4. The alpha-helix, beta-strand and random loop are in red, yellow and green, respectively. B, E: The predicted binding sites (blue) for PsTLR2-1 and PsTLR4 proteins. C: Homology model of human HsTLR2 (red), mouse MmTLR2 (light blue) and chicken GgTLR2-1 (blue) aligned with PsTLR2-1 (green). F: Homology model of human HsTLR4 (red), mouse MmTLR4 (light blue) and chicken GgTLR4 (yellow) aligned with PsTLR4 (green). (For interpretation of the references to colour in this figure legend, the reader is referred to the Web version of this article.)

PsTNF, as the important components in TLR-mediated immune responses, were found to be susceptible to bacterial stress and exhibited up-regulated expression levels under *A. hydrophila* challenge. These findings will facilitate the further exploration of PsTLR roles in regulating the immune system of *P. sinensis*.

Author contributions

T.L. and H.Z. conceived and designed the study. T.L. and S.C. were responsible for data analysis. T.L. and Y.H. carried out the gene expression analysis. T.L. wrote the manuscript. T.L., S.C. and H.Z. revised the manuscript. All authors read and approved the final manuscript.

Competing interests

The authors declare that they have no competing interests.

Acknowledgements

This work was supported by grants from the Doctoral Scientific Research Fund of Northwest A&F University (2452017213), PR-China.

Appendix A. Supplementary data

Supplementary data to this article can be found online at https://doi.org/10.1016/j.fsi.2019.01.052.

References

[1] S. Akira, S. Uematsu, O. Takeuchi, Pathogen recognition and innate immunity, Cell 124 (4) (2006) 783–801.
[2] T. Kawai, S. Akira, The role of pattern-recognition receptors in innate immunity: update on Toll-like receptors, Nat. Immunol. 11 (5) (2010) 373–384.
[3] A.P. West, A.A. Koblansky, S. Ghosh, Recognition and signaling by toll-like receptors, Annu. Rev. Cell Dev. Biol. 22 (2006) 409–437.
[4] L.A. O'Neill, D. Golenbock, A.G. Bowie, The history of Toll-like receptors redefining innate immunity, Nat. Rev. Immunol. 13 (6) (2013) 453–460.
[5] J. Wang, Z. Zhang, J. Liu, J. Zhao, D. Yin, Ectodomain architecture affects sequence and functional evolution of vertebrate toll-like receptors, Sci. Rep. 6 (2016) 26705.
[6] T. Hibino, M. Loza-Coll, C. Messier, A.J. Majeske, A.H. Cohen, D.P. Terwilliger, K.M. Buckley, V. Brockton, S.V. Nair, K. Berney, S.D. Fugmann, M.K. Anderson, Z. Pancer, R.A. Cameron, L.C. Smith, J.P. Rast, The immune gene repertoire encoded in the purple sea urchin genome, Dev. Biol. 300 (1) (2006) 349–365.
[7] J.P. Rast, C. Messier-Solek, Marine invertebrate genome sequences and our evolving understanding of animal immunity, Biol. Bull. 214 (3) (2008) 274–283.
[8] N. Sasaki, M. Ogasawara, T. Sekiguchi, S. Kusumoto, H. Satake, Toll-like receptors of the ascidian, *Ciona intestinalis*: prototypes with hybrid functionalities of vertebrate Toll-like receptors, J. Biol. Chem. 284 (40) (2009) 27336–27343.
[9] H. Satake, T. Sekiguchi, Toll-like receptors of deuterostome invertebrates, Front. Immunol. 3 (2012) 34.
[10] J.C. Roach, G. Glusman, L. Rowen, A. Kaur, M.K. Purcell, K.D. Smith, L.E. Hood, A. Aderem, The evolution of vertebrate Toll-like receptors, Proc. Natl. Acad. Sci. U.S.A. 102 (27) (2005) 9577–9582.
[11] M.H. Solbakken, O.K. Tørresen, A.J. Nederbragt, M. Seppola, T.F. Gregers, K.S. Jakobsen, S. Jentoft, Evolutionary redesign of the Atlantic cod (*Gadus morhua* L.) Toll-like receptor repertoire by gene losses and expansions, Sci. Rep. 6 (2016) 25211.
[12] Z. Zhang, H.J. Schluesener, Mammalian toll-like receptors: from endogenous ligands to tissue regeneration, Cell. Mol. Life Sci. 63 (24) (2006) 2901–2907.
[13] O. Takeuchi, K. Hoshino, S. Akira, Cutting edge: TLR2-deficient and MyD88-deficient mice are highly susceptible to *Staphylococcus aureus* infection, J. Immunol. 165 (10) (2000) 5392–5396.

[14] J.H. Wang, M. Doyle, B.J. Manning, Q.D. Wu, S. Blankson, H.P. Redmond, Induction of bacterial lipoprotein tolerance is associated with suppression of toll-like receptor 2 expression, J. Biol. Chem. 277 (39) (2002) 36068–36075.

[15] D. Hanzelmann, H.S. Joo, M. Franz-Wachtel, T. Hertlein, S. Stevanovic, B. Macek, C. Wolz, F. Götz, M. Otto, D. Kretschmer, A. Peschel, Toll-like receptor 2 activation depends on lipopeptide shedding by bacterial surfactants, Nat. Commun. 7 (2016) 12304.

[16] C. Shen, A.D. Shen, Identification of a novel transcript of human MD2 gene, Gene 590 (1) (2016) 123–127.

[17] Y. Zhou, Q. Liang, W. Li, Y. Gu, X. Liao, W. Fang, X. Li, Characterization and functional analysis of toll-like receptor 4 in Chinese soft-shelled turtle *Pelodiscus sinensis*, Dev. Comp. Immunol. 63 (2016) 128–135.

[18] S. Shang, H. Zhong, X. Wu, Q. Wei, H. Zhang, J. Chen, Y. Chen, X. Tang, H. Zhang, Genomic evidence of gene duplication and adaptive evolution of Toll like receptors (TLR2 and TLR4) in reptiles, Int. J. Biol. Macromol. 109 (2018) 698–703.

[19] T. Liu, X. Chu, Y. Huang, P. Yang, Q. Li, L. Hu, H. Chen, Q. Chen, Androgen-related sperm storage in oviduct of Chinese Soft-Shelled Turtle *in vivo* during annual cycle, Sci. Rep. 6 (2016) 20456.

[20] L.M. Zimmerman, L.A. Vogel, R.M. Bowden, Understanding the vertebrate immune system: insights from the reptilian perspective, J. Exp. Biol. 213 (5) (2010) 661–671.

[21] J. Chen, X. Ding, N. Zhu, L. Kong, Z. He, Prevalence and antimicrobial susceptibility of Aeromonas, species from diseased Chinese soft-shelled turtles (*Trionyx sinens*), Aquacult. Res. 46 (6) (2013) 1527–1536.

[22] Q. Shan, G. Zheng, S. Liu, Y. Bai, L. Li, Y. Yin, L. Ma, X. Zhu, Pharmacokinetic/pharmacodynamic relationship of marbofloxacin against *Aeromonas hydrophila* in Chinese soft-shelled turtles (*Trionyx sinensis*), J. Vet. Pharmacol. Therapeut. 38 (6) (2015) 537–542.

[23] X. Zhou, Q. Guo, H. Dai, Identification of differentially expressed immune-relevant genes in Chinese soft-shelled turtle (*Trionyx sinensis*) infected with *Aeromonas hydrophila*, Vet. Immunol. Immunopathol. 125 (1–2) (2008) 82–91.

[24] J. Chen, N. Zhu, L. Kong, Y. Bei, T. Zheng, X. Ding, Z. He, First case of soft shell disease in Chinese soft-shelled turtle (*Trionyx sinens*) associated with *Aeromonas sobria-A. veronii* complex, Aquaculture 406 (2013) 62–67.

[25] P.R. Rauta, M. Samanta, H.R. Dash, B. Nayak, S. Das, Toll-like receptors (TLRs) in aquatic animals: signaling pathways, expressions and immune responses, Immunol. Lett. 158 (1–2) (2014) 14–24.

[26] Z. Wang, J. Pascual-Anaya, A. Zadissa, W. Li, Y. Niimura, Z. Huang, C. Li, S. White, Z. Xiong, D. Fang, B. Wang, Y. Ming, Y. Chen, Y. Zheng, S. Kuraku, M. Pignatelli, J. Herrero, K. Beal, M. Nozawa, Q. Li, J. Wang, H. Zhang, L. Yu, S. Shigenobu, J. Wang, J. Liu, P. Flicek, S. Searle, J. Wang, S. Kuratani, Y. Yin, B. Aken, G. Zhang, N. Irie, The draft genomes of soft-shell turtle and green sea turtle yield insights into the development and evolution of the turtle-specific body plan, Nat. Genet. 45 (6) (2013) 701–706.

[27] T. Liu, P. Yang, H. Chen, Y. Huang, Y. Liu, Y. Waqas, N. Ahmed, X. Chu, Q. Chen, Global analysis of differential gene expression related to long-term sperm storage in oviduct of Chinese Soft-Shelled Turtle *Pelodiscus sinensis*, Sci. Rep. 6 (2016) 33296.

[28] T. Liu, L. Wang, H. Chen, Y. Huang, P. Yang, A. Nisar, T. Wang, Y. Liu, Q. Chen, Molecular and cellular mechanisms of apoptosis during dissociated spermatogenesis, Front. Physiol. 8 (2017) 188.

[29] L. Hu, Q. Li, P. Yang, J.A. Gandahi, T.S. Arain, Y. Le, Q. Zhang, T. Liu, M.Y. Waqas, N. Ahmad, Y. Liu, Q. Chen, Expression of TLR2/4 on epididymal spermatozoa of the Chinese soft-shelled turtle *Pelodiscus sinensis* during the hibernation season, Anat. Rec. 299 (11) (2016) 1578–1584.

[30] X. Li, B. Zhu, N. Chen, H. Hu, J. Chen, X. Zhang, J. Li, W. Fang, Molecular characterization and functional analysis of MyD88 in Chinese soft-shelled turtle *Trionyx sinensis*, Fish Shellfish Immunol. 30 (1) (2011) 33–38.

[31] S. Kumar, G. Stecher, K. Tamura, MEGA7: molecular evolutionary genetics analysis version 7.0 for bigger datasets, Mol. Biol. Evol. 33 (7) (2016) 1870–1874.

[32] L.A. Kelley, S. Mezulis, C.M. Yates, M.N. Wass, M.J. Sternberg, The Phyre2 web portal for protein modeling, prediction and analysis, Nat. Protoc. 10 (6) (2015) 845–858.

[33] M.N. Wass, L.A. Kelley, M.J. Sternberg, 3DLigandSite: predicting ligand-binding sites using similar structures, Nucleic Acids Res. 38 (2010) W469–W473.

[34] K.J. Livak, T.D. Schmittgen, Analysis of relative gene expression data using real-time quantitative PCR and the $2^{-\Delta\Delta CT}$ method, Methods 25 (4) (2001) 402–408.

[35] A.J. Saldanha, Java Treeview-extensible visualization of microarray data, Bioinformatics 20 (17) (2004) 3246–3248.

[36] K. Oda, H. Kitano, A comprehensive map of the toll-like receptor signaling network, Mol. Syst. Biol. 2 (2006) 0015.

[37] N. Matsushima, P. Enkhbayar, M. Kamiya, M. Osaki, R. Kretsinger, Leucine-rich repeats (LRRs): structure, function, evolution and interaction with ligands, Drug. Design Rev. 2 (4) (2005) 305–322.

[38] L.A. O'Neill, A.G. Bowie, The family of five: TIR-domain-containing adaptors in toll-like receptor signaling, Nat. Rev. Immunol. 7 (5) (2007) 353–364.

[39] J. Wang, Z. Zhang, J. Liu, F. Li, F. Chang, H. Fu, J. Zhao, D. Yin, Structural characterization and evolutionary analysis of fish-specific TLR27, Fish Shellfish Immunol. 45 (2) (2015) 940–945.

[40] Y. Wang, J. Li, J. Han, C. Shu, T. Xu, Identification and characteristic analysis of TLR28: a novel member of the TLR1 family in teleost, Dev. Comp. Immunol. 62 (2016) 102–107.

[41] H. Zhou, J. Gu, S.J. Lamont, X. Gu, Evolutionary analysis for functional divergence of the toll-like receptor gene family and altered functional constraints, J. Mol. Evol. 65 (2) (2007) 119–123.

[42] Q. Xing, H. Liao, X. Xun, J. Wang, Z. Zhang, Z. Yang, X. Huang, Z. Bao, Genome-wide identification, characterization and expression analyses of *TLRs* in Yesso scallop (*Patinopecten yessoensis*) provide insight into the disparity of responses to acidifying exposure in bivalves, Fish Shellfish Immunol. 68 (2017) 280–288.

[43] Y. Gong, S. Feng, S. Li, Y. Zhang, Z. Zhao, M. Hu, P. Xu, Y. Jiang, Genome-wide characterization of Toll-like receptor gene family in common carp (*Cyprinus carpio*) and their involvement in host immune response to *Aeromonas hydrophila* infection, Comp. Biochem. Physiol. Genom. Proteonom. 24 (2017) 89–98.

[44] C. Tong, Y. Lin, C. Zhang, J. Shi, H. Qi, K. Zhao, Transcriptome-wide identification, molecular evolution and expression analysis of Toll-like receptor family in a Tibet fish, *Gymnocypris przewalskii*, Fish Shellfish Immunol. 46 (2) (2015) 334–345.

[45] J. Zhang, Evolution by gene duplication: an update, Trends Ecol. Evol. 18 (6) (2003) 292–298.

[46] C.L. Mcgrath, M. Lynch, Evolutionary Significance of Whole-Genome Duplication-Polyploidy and Genome Evolution, Springer-Verlag, Berlin, 2012, pp. 1–20.

[47] Y. Van de Peer, S. Maere, A. Meyer, The evolutionary significance of ancient genome duplications, Nat. Rev. Genet. 10 (10) (2009) 725–732.

[48] J. Zhang, X.H. Kong, C.J. Zhou, L. Li, G.X. Nie, X.J. Li, Toll-like receptor recognition of bacteria in fish: ligand specificity and signal pathways, Fish Shellfish Immunol. 41 (2) (2014) 380–388.

[49] N.D. Temperley, S. Berlin, I. Paton, D.K. Griffin, D.W. Burt, Evolution of the chicken Toll-like receptor gene family: a story of gene gain and gene loss, BMC Genomics 9 (2008) 62.

[50] M.A. Opsal, D.I. Våge, B. Hayes, I. Berget, S. Lien, Genomic organization and transcript profiling of the bovine toll-like receptor gene cluster TLR6-TLR1-TLR10, Gene 384 (2006) 45–50.

[51] X.T. Zhang, G.R. Zhang, Z.C. Shi, Y.J. Yuan, H. Zheng, L. Lin, K.J. Wei, W. Ji, Expression analysis of nine Toll-like receptors in yellow catfish (*Pelteobagrus fulvidraco*) responding to *Aeromonas hydrophila* challenge, Fish Shellfish Immunol. 63 (2017) 384–393.

[52] J. Ao, Y. Mu, K. Wang, M. Sun, X. Wang, X. Chen, Identification and characterization of a novel Toll-like receptor 2 homologue in the large yellow croaker *Larimichthys crocea*, Fish Shellfish Immunol. 48 (2016) 221–227.

[53] Z. Qi, Q. Zhang, Z. Wang, T. Ma, J. Zhou, J.W. Holland, Q. Gao, Transcriptome analysis of the endangered Chinese giant salamander (*Andrias davidianus*): immune modulation in response to *Aeromonas hydrophila* infection, Vet. Immunol. Immunopathol. 169 (2016) 85–95.